# Substrate channeling in oxylipin biosynthesis through a protein complex in the plastid envelope of *Arabidopsis thaliana*

Stephan Pollmann[1,*], Armin Springer[2], Sachin Rustgi[3,4,5], Diter von Wettstein[4,5,6,†], ChulHee Kang[7-9], Christiane Reinbothe[10] and Steffen Reinbothe[10,*]

[1] Centro de Biotecnología y Genómica de Plantas, Universidad Politécnica de Madrid (UPM) – Instituto Nacional de Investigación y Tecnología Agraria y Alimentación (INIA), Campus de Montegancedo, 28223 Pozuelo de Alarcón (Madrid), Spain

[2] Medizinische Biologie und Elektronenmikroskopisches Zentrum (EMZ), Universitätsmedizin Rostock, D-18055 Rostock Germany

[3] Clemson University, Department of Plant and Environmental Sciences, Pee Dee Research and Education Center, Florence, SC 29506, USA

[4] Department of Crop and Soil Sciences, Washington State University, Pullman WA 99164, USA

[5] Molecular Plant Sciences Program, Washington State University, Pullman WA 99164, USA

[6] Center for Reproductive Biology, Washington State University, Pullman WA 99164, USA

[7] Department of Chemistry, Washington State University, Pullman WA 99164, USA

[8] School of Molecular Biosciences, Washington State University, Pullman WA 99164, USA

[9] Biomolecular Crystallography Center, Washington State University, Pullman WA 99164, USA

[10] Laboratoire de Bioénergétique Fondamentale et Appliquée, Université Grenoble Alpes, BP 53, Grenoble, Cedex F-38041, France

[†] Deceased April 13, 2017

[*] Correspondence: stephan.pollmann@upm.es or sreinbot@ujf-grenoble.fr

Centro de Biotecnología y Genómica de Plantas (UPM-INIA). Campus de Montegancedo. Autopista M40 (km 38), 28223 Pozuelo de Alarcón, Madrid, Spain

Phone: +34 913364589

Fax: 34-917157721

Running head: A protein complex involved in JA biosynthesis

---

Word count: 5159

Figures: 7

Supplementary data: FileI, includes 4 Figures; File II, includes: 9 Figures, 2 Tables.

## ABSTRACT

Oxygenated membrane fatty acid derivatives dubbed oxylipins play important roles in the plant's defense against biotic and abiotic cues. Plants challenged by insect pests, for example, synthesize a blend of different defense compounds that, amongst others, comprise volatile aldehydes and jasmonic acid (JA). Because all oxylipins are derived from the same pathway, we asked how their synthesis might be regulated and focused on two closely related, atypical cytochrome P450 enzymes designated CYP74A and CYP74B, i.e., allene oxide synthase (AOS) and hydroperoxide lyase (HPL). Both enzymes compete for the same substrate but give rise to different products. While the final product of the AOS branch is JA, those of the HPL branch comprise volatile aldehydes and alcohols. AOS and HPL are plastid envelope enzymes in *Arabidopsis thaliana* but accumulate at different locations. Biochemical experiments identified AOS as constituent of complexes also containing lipoxygenase 2 (LOX2) and allene oxide cyclase (AOC), which catalyze consecutive steps in JA precursor biosynthesis, while excluding the concurrent HPL reaction. Based on published X-ray data, the structure of this complex could be modelled and amino acids involved in catalysis and subunit interactions identified. Genetic studies identified the microRNA 319 (miR319)-regulated clade of TCP (TEOSINTE BRANCHED/CYCLOIDEA/PCF) transcription factor genes and CORONATINE INSENSITIVE 1 (COI1) to control JA production through the AOS-LOX2-AOC2 complex. Together, our results define a molecular branch point in oxylipin biosynthesis that allows fine-tuning the plant's defense machinery in response to biotic and abiotic stimuli.


***Key words*:** Allene oxide synthase (AOS); Allene oxide cyclase (AOC); Chloroplast envelope protein complex; Hydroperoxide lyase (HPL); Lipoxygenase (LOX); Metabolite channeling; Plant defense

## INTRODUCTION

Jasmonic acid (JA) and its derivatives are cyclopentanone compounds of widespread occurrence and ubiquitous function in plants (Böttcher and Pollmann, 2009; Reinbothe *et al.*, 2009; Wasternack and Hause, 2013; Yan *et al.*, 2013). JA biosynthesis comprises the release of linolenic acid from membrane lipids by phospho- and galactolipases, as well as 13-lipoxygenase (LOX), allene oxide synthase (AOS), and allene oxide cyclase (AOC) carrying out consecutive reactions in chloroplasts (Fig. 1). Whereas 13-LOX (EC 1.13.11.12) catalyzes the *regio*- and *stereo*specific hydroperoxidation of the C-13 atom of α-linolenic acid (α-LeA) giving rise to (13*S*)-hydroperoxylinolenic acid (13-HPOT), AOS (EC 4.2.1.92) converts 13-HPOT to 12,13-epoxylinolenic acid (EOT). Because EOT is short-lived and spontaneously disintegrates into volatile α- and γ-ketols as well as racemic 12-oxo-phytodienoic acid (OPDA), plants make use of AOC (EC 5.3.99.6) to assure *cis*-(+)-12-oxo-phytodienoic acid (*cis*-(+)-12-OPDA) synthesis. *cis*-(+)-12-OPDA then is exported from chloroplasts to the cytosol and transported further into peroxisomes, where the final reduction and ß-oxidation steps of JA biosynthesis take place. In *Arabidopsis thaliana*, six genes encode LOX isoforms, whereas one and four genes encode AOS and AOC enzymes, respectively. Mutant studies have provided valuable insights into the roles of the different LOX, AOS and AOC isoforms *in planta* (Schaller and Stintzi, 2009; Schaller *et al.*, 2008; Wasternack and Hause, 2013; Yan *et al.*, 2013).

(+)-*7-iso*-JA-Ile (JA-Ile) is the actual physiologically active compound (Fonseca *et al.*, 2009). It triggers changes in gene expression including the activation of defense genes and inhibition of photosynthetic genes (Reinbothe *et al.*, 1993a; Reinbothe *et al.*, 1993b; Rustgi *et al.*, 2014). Key regulatory elements in JA signaling involve the F-box protein COI1 (CORONATINE INSENSITIVE 1) acting as JA-Ile receptor (Xie *et al.*, 1998; Yan *et al.*, 2009), the E3 ubiquitin-ligase Skp-Cullin-F-box complex $SCF^{COI1}$, and the JASMONATE ZIM-domain (JAZ) transcriptional repressors normally suppressing expression of JA response genes (Chini *et al.*, 2007; Chung *et al.*, 2008; Thines *et al.*, 2007). Binding of JA-Ile to COI1 elicits the degradation of JAZ transcriptional repressors through the 26S proteasome and permits expression of JA response

genes, driven by a number of MYC transcription factors (Chini *et al.*, 2009; Fernández-Calvo *et al.*, 2011; Hoffmann *et al.*, 2011; Schweizer *et al.*, 2013).

The Vick and Zimmerman pathway through which JA is produced has a number of branch points (Fig. 1). The question of how the flow of metabolites through the different branches is regulated in time and space is largely unanswered. In particular, several reactions compete for 13-HPOT *in planta* (Griffiths, 2015; Nilsson *et al.*, 2016; Wasternack and Hause, 2013). One such reaction is catalyzed by fatty acid hydroperoxide lyase (HPL) that cleaves 13-HPOT into *Z*-3-hexenal and 12-oxo-*cis*-9-dodecenoic acid (ODA) of which c*is*-3-hexenal and the corresponding alcohol are volatile compounds operative in herbivore deterrence (Bate and Rothstein, 1998; Blée, 1998; Croft *et al.*, 1993; Wu and Baldwin, 2010)(Fig. 1). Here, we report on the identification of a protein complex comprising LOX2, AOS and AOC2 in the plastid envelope of *Arabidopsis* chloroplasts that channels α-LeA into JA biosynthesis. Because the expression of LOX2, AOS and AOC2 is under the control of JA-responsive microRNAs and *COI1*, a mechanism is suggested that boosts JA over aldehyde production for rapid local and systemic defense gene activation in plants.

## RESULTS

### In vitro-*import into chloroplasts and membrane targeting of AOS and HPL*

AOS and HPL from *Arabidopsis thaliana* and other plant species belong to the family of atypical cytochrome P450s, designated CYP74. AOS (CYP74A) and HPL (CYP74B) require neither $O_2$ nor NADPH-dependent cytochrome P450 reductase for activity and thus are non-canonical P450s (Froehlich *et al.*, 2001; Laudert *et al.*, 1996; Song and Brash, 1991). Previously described cDNAs for AtAOS and AtHPL (Froehlich *et al.*, 2001; Laudert *et al.*, 1996) were used for coupled *in vitro*-transcription/translation in wheat germ extracts. The $^{35}$S-methionine- or $^{14}$C-leucine-labeled proteins were then added to *Arabidopsis* chloroplasts that had been isolated by Percoll/sucrose density gradient centrifugation. Import experiments revealed that both AOS and HPL were taken up by isolated chloroplasts and processed by cleavage of their transit peptides (Fig. 2A). The resulting mature enzymes, however, were targeted to different locations (Fig.

2B-D). Whereas AOS was targeted to the inner envelope of chloroplasts, HPL was localized in the outer envelope fraction. Both enzymes were degraded by added trypsin, but only HPL was sensitive to thermolysin (Fig. 2A and B). Thermolysin is a protease that degrades surface-exposed proteins of the outer plastid envelope, whereas trypsin is known to access the intermembrane space between the outer and inner envelope, respectively (Cline *et al.*, 1984; Kessler and Blobel, 1996). Thus, AOS is likely to face the intermembrane space as it was protected against thermolysin, whereas HPL is exposed to the cytosolic side of the outer plastid envelope and was, thus, sensitive to thermolysin. Western blot experiments revealed the co-localization of AOS with two translocon proteins of the inner chloroplast envelope, TIC55 and TIC110, and that of HPL with the translocon protein of the outer chloroplast envelope, TOC75 (Fig. 2C). Using TIC110 as diagnostic marker, any post-import degradation of $^{35}$S-AOS or $^{35}$S-HPL could be excluded (Fig. 2B, panel c). TIC110 is a very sensitive marker for monitoring the trypsin digestion procedure and easily undergoes degradation if no precautions are taken, such as inclusion of trypsin inhibitor during all chloroplast fractionation steps (Jackson *et al.*, 1998). Extraction of outer and inner plastid envelopes with 1 M NaCl or 0.1 M $Na_2CO_3$, pH 11, revealed that HPL and AOS were tightly bound to their respective target membranes (Fig. 2D). The localizations of HPL and AOS confirmed previous data for chloroplasts from *Arabidopsis* (Joyard *et al.*, 2010; Mwenda et al., 2015) and tomato (Froehlich *et al.*, 2001), respectively, while not precluding divergent locations in other plant species.

***Isolation of plastid envelope proteins interacting with AOS and HPL***

We next attempted to identify proteins interacting with AOS in the envelope of *Arabidopsis* chloroplasts. COOH-terminal, hexa-histidine ($His_6$)-tagged AOS (AOS-$(His)_6$) was expressed in bacteria and purified to apparent homogeneity by Ni-NTA chromatography. The chemically pure protein was incubated with isolated chloroplasts in standard import reactions containing 2.5 mM Mg-ATP (Froehlich *et al.*, 2001). After incubation, mixed outer and inner envelopes were isolated from ruptured chloroplasts (Li *et al.*, 1991; Schnell *et al.*, 1994) and solubilized with 1.3% decyl maltoside (Caliebe *et al.*, 1997). Proteins adhering to

AOS-$(His)_6$ were subjected to size exclusion chromatography and AOS-$(His)_6$ detected with AOS-specific or $(His)_6$ antibodies (Froehlich *et al.*, 2001; Laudert *et al.*, 1996). For comparison, AOS-containing plastid envelope complexes were isolated from transgenic plants overexpressing Flag-tagged AOS (AOS–Flag) under the control of the 35S cauliflower mosaic virus promoter.

Figure 3A and B depict the elution profiles of AOS after its purification from either isolated chloroplasts following the *in vitro*-import reaction of AOS-$(His)_6$ or transgenic plants overexpressing Flag-tagged AOS. Whereas AOS-Flag and AOS-$(His)_6$ were present in higher molecular mass complexes of ≈250 kDa (peak I), a second, lower molecular mass complex was only detectable for AOS-Flag (peak II). The lack of a corresponding AOS-$(His)_6$ peak may be due to the lower abundance of this protein in the *in vitro*-uptake assays with isolated chloroplasts. When the total pattern of proteins that co-purified with AOS-$(His)_6$ in peak I was analyzed by SDS-PAGE, at least 10 bands were found (Fig. 3C, lane 1) of which, besides the bait protein, the ≈100 kDa band was identified by protein sequencing as LOX2 and the ≈72 kDa and ≈24 kDa bands as AOC2, forming SDS-resistant trimers and monomers, respectively. When similar experiments were carried out with HPL-$(His)_6$, a completely different protein pattern was obtained which, most notably, did not contain any of the proteins detected with AOS-$(His)_6$. (Fig. 3C, lane 2).

### *Genetic evidence for the existence of a chloroplast envelope complex comprising AOS, LOX2 and AOC2*

Because the expression of *LOX2*, *AOS* and *AOC2* in *Arabidopsis* is under the control of the microRNA 319 (miR319)-regulated clade of *TCP* (*TEOSINTE BRANCHED/CYCLOIDEA/PCF*) transcription factor genes (Schommer *et al.*, 2008), we used the *jaw*-D mutant with strongly reduced mi319-dependent expression of JA biosynthetic genes to investigate the interaction of LOX2, AOS and AOC2 genetically. When *jaw*-D plants, in which *TCP4* expression is strongly down-regulated, and primary transformants expressing a miR319-resistant version of *TCP4* (referred to as *TCP4* plants in the following) that dominantly regulates *LOX2* expression (Palatnik *et al.*, 2003; Schommer *et al.*,

2008), were grown for 14 d in a greenhouse, not much of a difference in phenotype was seen. However, this picture changed at later stages of plant development and especially at the stage when plants matured and entered senescence. In agreement with previous results (Schommer *et al.*, 2008), *TCP4* plants then displayed a marked acceleration of senescence, whereas *jaw*-D plants exhibited a tremendous, 2 week-delay in leaf senescence. These differential changes correlated with altered patterns of plastid envelope proteins comprising LOX2, AOS and AOC2 (Fig. 4; see also Supplemental Information file I showing respective densitometric analyses using the NIH endorsed ImageJ software, https://imagej.net/). *TCP4* plants more rapidly accumulated all three JA biosynthesis enzymes than wild-type plants (Fig. 4A)

JA biosynthesis is under the control of a feed-forward loop and consequently can be boosted by exogenously added JA (Wasternack and Hause, 2013; Yan *et al.*, 2013). To pinpoint the role of LOX2, AOS and AOC2 in this loop, JA-deficient seedlings of the *aos* mutant (Park *et al.*, 2002; von Malek *et al.*, 2002) and JA-Ile-insensitive seedlings of the *coi1* mutant (Feys *et al.*, 1994) were used. For comparison, we employed *Arabidopsis* mutants defective in the *LOX2* and *AOC2* gene, respectively (Seltmann *et al.*, 2010; Stenzel *et al.*, 2012). When the patterns of plastid envelope proteins were compared, some differential effects were observed. As displayed in Fig. 4B, the *aoc2* knock-out mutants contained wild-type levels of AOC1, AOC3 and AOC4 as well as wild-type levels of *AOS* and *LOX2*. By contrast, *aos* and *lox2* mutants likewise expressed reduced amounts of LOX2 and AOC2 trimers, while retaining the levels of AOC1-4 monomers. These findings were suggestive of partially overlapping roles and expression patterns of the four AOC family members (see Supplemental Information file II; Fig. S1-3), with AOC1, AOC3 and AOC4 presumably being capable of replacing AOC2 forming homo- and hetero-complexes. It has recently been demonstrated that all four AOCs display identical catalytic activities (Otto *et al.*, 2016).

To further dissect the feed-forward loop operating in JA biosynthesis, seedlings of the JA-insensitive *coi1* mutant (Feys *et al.*, 1994) and JA-resistant *jar1* mutant (Staswick *et al.*, 1992) were used. *JAR1* encodes an enzyme that

provides the physiologically active JA-Ile conjugate for CORONATINE INSENSITIVE 1 (COI1)-dependent signal transduction (Feys *et al.*, 1994; Staswick *et al.*, 1992). *coi1* and *jar1* seedlings were grown for 14 days in continuous white light and in turn sprayed with MeJA. MeJA treatment triggered expression of LOX2, AOS and AOC1-4 in wild-type plants but not in *jaw*-D, *coi1* and *jar1* plants (Fig. 4C). Hence, JA production was required and relied on an intact JA signal transduction chain comprising JA-Ile and COI1, linking JA signal with miR319-regulated TCPs.

***Probing the interaction of LOX2, AOS and AOC2 through crosslinking***

The presence of higher molecular mass complexes containing LOX2, AOS and AOC2 in the envelope of *Arabidopsis* chloroplasts suggested the possibility that the enzymes may physically and functionally interact in JA precursor biosynthesis. As a first step to test this hypothesis, crosslinking experiments were conducted using bacterially expressed, $(His)_6$-tagged, purified precursors that had been derivatized with $^{125}$I-N-4[(p-azidosalicyl-amido)butyl]-3´(2-pyridyl-dithio)propion-amide ($^{125}$I-APDP), which is a hetero-bifunctional, photoactivatable and cleavable label-transfer crosslinker frequently used in the chloroplast protein import field (e.g., Ma *et al.*, 1996). $^{125}$I-APDP contains a 21 Å spacer arm that, depending on its location on the bait protein, can penetrate to different extents into the respective target membrane and label proteins and lipids.

$^{125}$I-APDP-labeled LOX2, AOS and AOC2, respectively, were imported in darkness into isolated *Arabidopsis* chloroplasts (Springer et al, 2016; Figs. 2 and S4). After 15 min incubation, label-transfer crosslinking was induced by UV-light exposure on ice. Envelopes, in turn, were isolated from ruptured chloroplasts, solubilized with 3% SDS (Ma *et al.*, 1996), and $^{125}$I-APDP-labeled proteins detected by SDS-PAGE and autoradiography. Figure 5A revealed different banding patterns for the three labeled proteins. LOX2 and AOC2 (being present as a trimer), both interacted with AOS, with little or no direct interaction between the two of them. For $^{125}$I-APDP-AOS, label transfer occurred onto LOX2 and AOC2 (Fig. 5A; see also the densitometric scans in Supplemental Information file I). Interestingly, $^{125}$I-APDP-AOS gave rise to both, $^{125}$I-labeled AOC2 trimers

and monomers (Fig. 5A). AOC2 monomers were also seen in assay mixtures containing $^{125}$I-APDP-LOX2. This observation could be suggestive of a shuffling of monomers and trimers of AOC2 into the envelope complex. On the other hand, the nature of the chosen crosslinker and its topology on the bait protein may explain this result. Last but not least, it is also possible that substrate binding and conversion affected the interaction of LOX2, AOS and AOC2 and thereby had an impact on the crosslinking results.

With respect to the overlapping expression pattern of the *AOC* isogenes (see Supplemental Information file II; Figs. S2D and S3), we additionally asked whether the respective isoenzymes are capable of forming heteromeric complexes within the chloroplast, or whether complex formation is restricted to the formation of homomers. By using a bimolecular fluorescence complementation (BiFC) approach, it was possible to demonstrate that there are no restrictions in complex formation, as all possible interactions of AOC1–4 have been detected by fluorophore complementation in chloroplasts of *Arabidopsis* protoplasts (Fig. S2). These results are in agreement with recent data by Otto *et al.* (2016) who studied the capabilities of all four AOC isoforms to form trimers and how this may affect enzyme activity.

If LOX2, AOS and AOC2 were to structurally and functionally interact, they could provide the possibility of substrate channeling without concurrent side reactions in *cis*-(+)-12-OPDA synthesis from α-LeA. To address this possibility, bacterially expressed and purified, non-$^{125}$I-APDP-derivatized AOS-$(His)_6$ was imported into *Arabidopsis* chloroplasts. Then, the plastids were lysed and protein complexes containing AOS-$(His)_6$ isolated by affinity chromatography from 1.3% decyl maltoside-solubilized envelopes. For reference, SDS-dissociated and dialyzed envelope complexes containing the free LOX2, AOS and AOC2 in amounts identical to those in the intact complexes were used. Activity measurements using α-LeA and 13-HPOT revealed a tight channeling of metabolites in the intact envelope complex. This is apparent from time courses of *cis*-(+)-12-OPDA formation from α-LeA and 13-HPOT (Fig. 5B) and respective quantification of *cis*-(+)-12-OPDA (Fig. 5C). While α-LeA was converted to *cis*-(+)-12-OPDA by the isolated, intact (non-SDS-dissociated) plastid envelope

complex, 13-HPOT was not accepted as substrate. In line with the tight channeling of metabolites, the AOC inhibitor vernolic acid ((+/-)-cis-12,13-epoxy-9(Z)-octadecenoic acid) (Hofmann *et al.*, 2006) was unable to impede *cis*-(+)-12-OPDA synthesis (Fig. 5C). When applied to the SDS-dissociated, dialyzed complex containing free LOX2, AOS and AOC2, however, vernolic acid did block *cis*-(+)-12-OPDA synthesis from α-LeA and 13-HPOT (Fig. 5C). Remarkably, the rate of *cis*-(+)-12-OPDA formation from α-LeA in the intact complex was 120-fold higher than that in the free-enzyme assay (Fig. 5C), suggesting tight functional LOX2-AOS-AOC2 interactions to occur and to boost *cis*-(+)-12-OPDA synthesis. In summary, we obtained 2-fold higher activities for the free-enzyme assay as compared to Otto *et al.* (2016), i.e., 5 nmoles OPDA per $min^{-1}$ $\mu g^{-1}$ AOC2 and a 240-fold greater activity for the complex-containing assay (600 nmoles OPDA per $min^{-1}$ $\mu g^{-1}$ AOC2).

***Interaction of LOX2, AOS and AOC2 probed in the Split-Ubiquitin system***

As an independent approach to confirm the interaction of LOX2, AOS and AOC2, we carried out split-ubiquitin yeast two-hybrid screens for membrane bound proteins. Yeast cells (strain DSY1) were first transformed with AOS- and LOX2-containing bait-vectors (AOS-Cub, LOX2-Cub), respectively, which express the bait proteins fused to the C-terminal part of UBIQUITIN. For each bait protein, we constructed and tested three different vectors (pAMBV4, pCMBV4, pTMBV4), providing promoters of different strength to drive bait protein expression. In our hands, the pTMBV4 vector that contains a highly potent TEF1 promoter gave the clearest results. Co-transformation was accomplished in a second, separate step in which AOS- and AOC2-containing prey vectors were introduced into the selected yeast cells (NubG-AOS, NubG-AOC2). As prey vectors, we used constructs that added the N-terminal part of UBIQUITIN to the N-terminal extremity of the preys (pADSL-Nx). In addition to the specific constructs used to study potential LOX2-AOS-AOC2-interactions, we used control vectors provided with the system to test for unspecific and auto-activation, respectively (NubG-Alg5), as well as positive (Alg5-Cub, NubI-Alg5) and negative (Alg5-Cub, NubG-Alg5) system controls. The co-transformed yeast cells were subjected to qualitative His-complementation growth tests carried out on SD

plates supplemented with 5 mM 3-AT (3-amino-1,2,4-triazole) lacking the three amino acids Leu, Trp, and His. Additionally, the relative ß-galactosidase activities of the investigated co-transformed yeast strains were determined to provide quantitative data on the interaction strength of the analyzed protein pairs. According to the results summarized in Fig. 6, interactions were observed between AOS and AOC2, with a fraction of AOS presumably forming dimers, as found for AOS from *Parthenium argentatum* (Chang *et al.*, 2008; Li *et al.*, 2008). Some interactions could also be detected for LOX2 with AOC2 and AOS, although these were quite variable and dependent on the respective bait and prey protein.

## DISCUSSION

### *Sequestration of jasmonate precursor biosynthesis through a protein complex in the plastid envelope*

In the present study, evidence is provided for the existence of a protein complex involved in JA precursor biosynthesis in *Arabidopsis* chloroplasts. We show that LOX2, AOS and AOC2, the enzymes that catalyze consecutive steps in JA precursor biosynthesis (Fig. 1), are co-localized in the inner envelope of *Arabidopsis* chloroplasts (Figs. 2 and S4; see also Springer et al., 2016), and formed complexes operating in *cis*-(+)-12-OPDA synthesis from α-LeA (Figs. 3, 5 and S5). It was possible to reconstitute a similar complex *in vitro* from soluble LOX2, AOS and AOC2 enzymes and isolated plastid envelope lipids (Fig. S5). In either case, LOX2, AOS and AOC2 were present in a 1:1:4 stoichiometry, indicating that these complexes may contain both, AOC2 monomers and trimers. The significance of this observation and the possibility of activity regulation through hetero-trimerization of AOC2 with AOC1, 3 and 4 remains to be established. It must be noted in this context, however, that also Zerbe and co-workers used AOS and AOC2 at a 1:4 molar ratio (Zerbe *et al.*, 2007). Interaction studies in the split-ubiquitin yeast two-hybrid system confirmed the interaction of AOS and AOC2 (Fig. 6). When isolated plastid envelope complexes were supplied with α-LeA, only *cis*-(+)-12-OPDA accumulated in the reaction medium (Fig. 5). No evidence was obtained for the release of significant amounts of HPOT or EOT and its short-lived disintegration products (α-ketols and γ-ketols) as well as of racemic OPDA into the reaction

mixture. These findings are suggestive of a tight channeling of metabolites through both, the isolated and reconstituted protein complexes. By virtue of the observed channeling of metabolites, the dilution of the reaction intermediates was kept low. On the other hand, the observed channeling of metabolites tremendously increased the rate of formation and, thus, yield of *cis*-(+)-12-OPDA from α-LeA. Compared to the free-enzyme assay, 120-fold higher activities were measured in the isolated envelope complex. Our data confirm and extend previous findings by Zerbe and colleagues who reconstituted *cis*-(+)-12-OPDA synthesis from 13-HPOT by combining purified recombinant AOS and AOC2 *in vitro* (Zerbe *et al.*, 2007). The authors found that both soluble and matrix-bound enzymes are active and that their co-fixation on a solid matrix increased the yield of *cis*-(+)-OPDA from 13-HPOT by about 50%. In contrast to these studies, however, in which AOS and AOC2 were randomly bound to the matrix, thus excluding tight substrate channeling, in our experiments the enzymes were orderly associated, thereby allowing the channeling of α-LeA. Because vernolic acid failed to inhibit *cis*-(+)-12-OPDA synthesis from α-LeA or 13-HPOT in the native and reconstituted complexes (Fig. 5, Fig. S5), we conclude that the active site of AOC2 is largely inaccessible to the inhibitor. On the other hand, exogenously administered 13-HPOT was not accepted as substrates for *cis*-(+)-12-OPDA synthesis by the native and reconstituted complexes, but it was accepted in case of the free-enzyme assay (Fig. 5C). On the basis of these results we conclude that *cis*-(+)-12-OPDA synthesis from α-LeA is strictly compartmentalized, presumably to prevent competing side reactions such as that from 13-HPOT catalyzed by HPL or by chemical decay, which give rise to α- and γ-ketols. By this means, plants avoid the costly formation of *n*-hexenal and 12-oxo acids implicated in direct and indirect defenses of herbivores (Hoffmann *et al.*, 2011; Wu and Baldwin, 2010), while maintaining the capacity to respond to biotic foes and abiotic stresses (Wasternack and Hause, 2013; Yan *et al.*, 2013).

### *Structural modeling of the LOX2-AOS-AOC2 envelope complex*

We conclude from our results that AOS forms complexes with both LOX2 and AOC2 *in planta* as well as *in vitro*. Molecular modeling was carried out to obtain

406 insight into the potential structure of this complex, using published X-ray struc-
407 ture data for soybean lipoxygenase L3 (PDB ID 1LNH;; Skrzypczak-Jankun *et*
408 *al.*, 1997; Youn et al., 2006), AOS (D 3CLI; Lee *et al.*, 2008) and AOC2 (PDB ID
409 2GIN; Hofmann *et al.*, 2006), obtained at 2.60 Å, 1.80 Å and 1.80 Å resolution,
410 respectively, as templates (Figs. S6-S8). First, homology modelling was done
411 for LOX2, based on the X-ray structure of soybean LOX L3 (Cho and Stahelin,
412 2006; Youn et al., 2006). The established LOX2 structure of Arabidopsis (Fig.
413 S6) was then used in modelling of the whole, LOX2-, AOS- and AOC2-contain-
414 ing complex. The top rank model depicted in Fig. 7 suggests that at least two
415 amino acid residues, Ser92 and Gly94, of LOX2 are potentially involved in the
416 LOX2-AOS interaction, forming hydrogen bonds with Ser272 of AOS (Fig. S9A).
417 The interacting Ser and Gly residues of LOX2 are not conserved between LOX2
418 and soybean LOX3 and reside in a loop region between β-sheets 1 and 2 of
419 LOX2. Similarly, one region of interacting amino acids could be identified for
420 each of the hypothetical LOX2-AOC2 and AOS-AOC2 complexes. In these
421 complexes, Asp96 of LOX2 is predicted to interact with Asn42 of AOC2, and
422 Phe44 and Ser45 of AOC2 were found when analyzing these enzymes apart
423 from LOX2, while not seeing them in the modeled LOX2-AOS-AOC2 complex
424 (Fig. S9B). Along with the crosslinking data, these findings are suggestive of a
425 dynamic equilibrium of binding and release of all three enzymes to and from the
426 complex.
427
428 Details of how the LOX2-AOS-AOC2 complex may be bound to the
429 membrane remain elusive. The fact that a functional complex could reconsti-
430 tuted from soluble LOX2, AOS and AOC2 enzyme molecules at first glance sug-
431 gests that the lipid bilayers might be dispensable for formation of the whole
432 complex. Nevertheless, all three enzymes attained salt- and protease-resistant
433 states after respective *in vitro*-import reactions with chloroplasts, suggesting
434 their tight binding to the lipid bilayers of the inner plastid envelope. Hydrophobic
435 transmembrane (TM) domains may anchor LOX2, AOS and AOC2 in the mem-
436 brane. Lee et al. (2008) identified several non-polar detergent binding α-helices
437 in AOS of which those designated α-F and α-G were tentatively defined as puta-
438 tive TM domains in our structural models (Fig. S7A). Predictions made with
439 TMpredn however, suggest a different part of the AOS polypeptide to form a

single TM domain and that this overlaps with some of the active site residues (Fig. S7B). Such overlap would resemble that in the AOC2 trimer where some active site residues appear to be embedded into/are part of the predicted TM domain (Fig. S8). However, it cannot be excluded that some of the hydrophobic β-sheets forming the characteristic beta-barrel cavity are involved in membrane binding (Fig. S8). Lastly, the LOX structure of Skrzypczak-Jankun et al. (1997) used for modelling LOX2 from *Arabidopsis* (Fig. S6) suggests a hydrophobic environment of the catalytic pocket that could overlap with the predicted TM domain. Further work is needed to resolve the structure of the LOX2-AOS-AOC2 complex and elucidate its membrane binding.

It is attractive to hypothesize that LOX2 and AOS compete for binding sites on AOC2, thereby provoking the formation of AOC trimers, possibly involving other available AOC isoforms, too (Hofmann and Pollmann, 2008; Hofmann *et al.*, 2006; Otto *et al.*, 2016). As described by Otto *et al.* (2016), trimerization of AOC isoenzymes is likely to contribute to activity regulation. Several salt bridges between monomers and a hydrophobic core within the AOC2 trimer were identified and functionally proven by site-directed mutagenesis. While Lys152 of one monomer and Glu128 of the neighboring monomer established the observed salt bridges, amino acids involved in building the hydrophobic core of the trimer comprised Leu40, Leu50, Leu53 and Ile79 of all three monomers (Otto *et al.*, 2016). Notable are the conservation of interacting amino acids and the overlapping expression patterns of AOC1/2 during germination, leaf production, rosette growth, inflorescence emergence and flowering with each other and with those of LOX2 and AOS (Fig. S1-3). By contrast, the expression pattern of AOC3 and AOC4 is more distinct (Fig. S1-3). On the other hand, HPL expression is comparably low in all of the developmental stages analyzed (Fig. S3). Together, these correlative data are suggestive of a co-evolution of mechanisms that allow favoring JA precursor biosynthesis over volatile production during plant development. This situation obviously changes when plants are challenged by chewing insects and trigger both direct and indirect defenses through the HPL pathway (Bate and Rothstein, 1998; Blée, 1998; Croft *et al.*, 1993; Wu and Baldwin, 2010). In functional terms, both AOS and HPL belong to the same superfamily of non-canonical cytochrome P450 enzymes but yet their amino

acid sequences are distinct enough to permit their unique reaction mechanisms (Lee et al., 2008). While AOS interacts with LOX2 and AOC2, no interacting partners could be identified for HPL (Fig. 3). Last but not least, the chloroplast localization of AOS and HPL is quite distinct and helps to assure that AOS operates in the channeling of α-LeA to OPDA, whereas HPL drives volatile production.

In agreement with previous publications (Gilbert *et al.*, 2008; Spivey and Ovádi, 1999), we conclude that compartmentalization of enzymes as well as organization into multi-protein complexes provides a highly specific cellular mechanism for controlling the flow of metabolites through key regulatory pathways and preventing unfavorable competing reactions. Work is in progress to obtain X-ray structural data for the identified LOX2-AOS-AOC2 complex from higher plant chloroplasts.

## EXPERIMENTAL PROCEDURES

*Plant growth*

Wild-type *Arabidopsis*, *jaw*-D (Palatnik *et al.*, 2003; Schommer *et al.*, 2008), *aos* (Park *et al.*, 2002; von Malek *et al.*, 2002), *coi1* (Feys *et al.*, 1994), *lox2* (Seltmann *et al.*, 2010), *aoc2* (Stenzel *et al.*, 2012) and *jar1* (Staswick *et al.*, 1992) genotypes were used in this study. Homozygous *aos* plants were obtained by hand pollinating flowers with *aos* plants that had been generated by spraying flowering homozygous plants with 45 µM methyl jasmonate (MeJA). Seeds from an $F_2$ population segregating for the *coi1* mutation were obtained as described (Feys *et al.*, 1994). Plants were grown at 25 °C under standard conditions either under continuous white light illumination provided by fluorescent bulbs (30 W/m$^2$) or 16 h light/8 h dark cycles.

*Generation of transgenic lines expressing AOS with COOH-terminally $(His)_6$ or FLAG tags*

Transgenic plants were generated expressing COOH-terminally $(His)_6$ or FLAG-tagged AOS as described in the Supplemental Information section and used for affinity purification of proteins interacting with AOS *in planta*.

*Production of proteins and import into chloroplasts*

Complementary DND (cDNA) clones for *AOS* (Laudert *et al.*, 1996) and *HPL* (Froehlich *et al.*, 2001) were cloned into appropriate vectors, allowing for their purification as $(His)_6$- or Flag-tagged proteins. For routine chloroplast import assays, $^{35}$S-methionine- or $^{14}$C-leucine-labeled proteins were produced by coupled *in vitro* transcription/translation in wheat germ extracts. Radiolabeled proteins were added to 50 µL import assays consisting of 25 µL of doubly-concentrated import buffer, 10 µL of a plastid suspension containing 5 x $10^7$ *Arabidopsis* chloroplasts, and 2.5 mM Mg-ATP. All import reactions were performed at 23 °C for 15 min in darkness. Post-import protease treatment of plastids with thermolysin or trypsin and extraction of membranes with sodium carbonate, pH 11, or 1 M NaCl were carried out as described (Cline *et al.*, 1984; Kessler and Blobel, 1996). Trypsin quenching was monitored by Western blotting using TIC110 as diagnostic marker and employing a trypsin inhibitor (Jackson *et al.*, 1998). Plastid sub-fractionation into envelopes, stroma and thylakoids was made according to Li et al. (1991). Protein was extracted and precipitated with trichloroacetic acid (5% (w/v) final concentration), resolved by SDS-PAGE on 10-20 % (w/v) polyacrylamide gradients (Laemmli, 1970) and detected by autoradiography.

*Isolation of AOS-containing higher molecular mass complexes*

AOS-$(His)_6$ was imported into isolated *Arabidopsis* chloroplasts and AOS-$(His)_6$ complexes released with detergent. For comparison, AOS-containing complexes were purified from plants expressing Flag-tagged AOS (AOS-Flag; see SI section). Both types of complexes, in turn, were subjected to size exclusion chromatography on Superose 6 (column model HR10/10, GE Healthcare) and individual fractions harvested and traced for the presence of AOS by Western blotting using AOS- or FLAG-specific antibodies (Laudert *et al.*, 1996) and an enhanced chemiluminescence kit (ECL, GE Healthcare).

*Crosslinking*

Crosslinking was carried out using $^{125}$I-*N*-[4[(p-azidosalicyl-amido)butyl]-3´(2-pyridyldithio) propionamid ($^{125}$I-APDP)-derivatized precursors, essentially as previously described (Ma *et al.*, 1996). Final protein samples were separated by reducing or non-reducing SDS-PAGE and $^{125}$I-labeled proteins detected by autoradiography.

*Enzyme activity measurements*

Activity measurements using the isolated native and reconstituted complexes or free enzymes were carried out as described in *Supplemental Materials*. HPLC and GC-MS analyses used to identify and quantify substrates and products of the LOX2, AOS and AOC2 reactions were performed according to Holtman *et al.* (1997) and Zerbe *et al.* (2007). Capillary chiral GC analysis was used to demonstrate the optical purity of the *cis*-(+)-enantiomer (>95%) that was reconfirmed by TLC, HPLC and GC analyses with a synthetic standard (Zerbe *et al.*, 2007).

*Yeast two-hybrid screens*

Split-ubiquitin yeast two-hybrid screens for membrane bound proteins were carried out according to the manufacturer's instructions using a commercial system (Dualsystems Biotech AG, Switzerland). Vector construction is described in *Supplemental Materials*.

*Bimolecular fluorescence complementation*

The BiFC experiments were carried out according to (Walter *et al.*, 2004). Vector construction and protoplast transformation is summarized in *Supplemental Materials*.

*Molecular modelling*

Molecular modeling methods and tools are described in the *Supplemental Material* section.

*Miscellaneous*

Western blotting was carried out according to (Towbin *et al.*, 1979), using the indicated antisera and enhanced chemiluminescence (ECL, GE Healthcare) or anti-rabbit, anti-goat, alkaline phosphatase systems.

ACKNOWLEDGMENTS

We are grateful to John Froehlich, Michigan State University, East Lansing, USA, Jörg Lehmann, formerly at Leibnitz Institute of Plant Biochemistry, Halle/Saale, Germany, Klaus Apel, formerly at Institute for Plant Sciences, ETH Zurich, Zurich, Switzerland, as well as Felix Kessler, Université Neuchatel, Neuchatel, Switzerland, and Danny J. Schnell, The University of Massachusetts, Amherst, USA, for gifts of cDNA clones and antibodies. The authors are also grateful to Nikolaus Amrhein, ETH Zurich, Zurich, Switzerland, for critically reviewing the manuscript and for his valuable comments. We thank Maik Hoffmann, Ruhr University Bochum, Germany, for technical assistance. This work was supported by a Marie-Curie grant of the European Communion [FP7-PEOPLE-CIG-2011-303744 to SP].

589 **REFERENCES**

590 Bate NJ, Rothstein SJ. 1998. C6-volatiles derived from the lipoxygenase
591 pathway induce a subset of defense-related genes. Plant Journal 16, 561-569.

592 Blée E. 1998. Phytooxylipins and plant defense reactions. Prog Lipid Res 37,
593 33-72.

594 Böttcher C, Pollmann S. 2009. Plant oxylipins: plant responses to 12-oxo-
595 phytodienoic acid are governed by its specific structural and functional
596 properties. FEBS Journal 276, 4693-4704.

597 Caliebe A, Grimm R, Kaiser G, Lubeck J, Soll J, Heins L. 1997. The
598 chloroplastic protein import machinery contains a Rieske-type iron-sulfur cluster
599 and a mononuclear iron-binding protein. EMBO Journal 16, 7342-7350.

600 Chang Z, Li L, Pan Z, Wang X. 2008. Crystallization and preliminary X-ray
601 analysis of allene oxide synthase, cytochrome P450 CYP74A2, from
602 Parthenium argentatum. Acta Crystallogr Sect F Struct Biol Cryst Commun 64,
603 668-670.

604 Chini A, Boter M, Solano R. 2009. Plant oxylipins: COI1/JAZs/MYC2 as the core
605 jasmonic acid-signalling module. FEBS Journal 276, 4682-4692.

606 Chini A, Fonseca S, Fernandez G, Adie B, Chico JM, Lorenzo O, Garcia-
607 Casado G, Lopez-Vidriero I, Lozano FM, Ponce MR. 2007. The JAZ family of
608 repressors is the missing link in jasmonate signalling. Nature 448.

609 Cho W, Stahelin RV. 2006. Membrane binding and subcellular targeting of C2
610 domains. Biochimica et Biophysica Acta 1761, 838-849.

611 Chung HS, Koo AJ, Gao X, Jayanty S, Thines B, Jones AD, Howe GA. 2008.
612 Regulation and function of Arabidopsis JASMONATE ZIM-domain genes in
613 response to wounding and herbivory. Plant Physiology 146, 952-964.

614 Cline K, Werner-Washburne M, Andrews J, Keegstra K. 1984. Thermolysin is a
615 suitable protease for probing the surface of intact pea chloroplasts. Plant
616 Physiology 75, 675-678.

617 Corey EJ, Matsuda SPT, Nagata R, Cleaver MB. 1988. Biosynthesis of 8-R-
618 HPETE and preclavulone-A from arachidonate in several species of caribbean

619 coral. A widespread route to marine prostanoids. Tetrahedron Letters 29, 2555-
620 2558.

621 Croft K, Jüttner F, Slusarenko AJ. 1993. Volatile Products of the Lipoxygenase
622 Pathway Evolved from *Phaseolus vulgaris* (L.) Leaves Inoculated with
623 *Pseudomonas syringae* pv *phaseolicola*. Plant Physiology 101, 13-24.

624 Fernández-Calvo P, Chini A, Fernandez-Barbero G, Chico JM, Gimenez-Ibanez
625 S, Geerinck J, Eeckhout D, Schweizer F, Godoy M, Franco-Zorrilla JM, Pauwels
626 L, Witters E, Puga MI, Paz-Ares J, Goossens A, Reymond P, De Jaeger G,
627 Solano R. 2011. The *Arabidopsis* bHLH Transcription Factors MYC3 and MYC4
628 Are Targets of JAZ Repressors and Act Additively with MYC2 in the Activation
629 of Jasmonate Responses. The Plant Cell 23, 701-715.

630 Feys B, Benedetti CE, Penfold CN, Turner JG. 1994. Arabidopsis Mutants
631 Selected for Resistance to the Phytotoxin Coronatine Are Male Sterile,
632 Insensitive to Methyl Jasmonate, and Resistant to a Bacterial Pathogen. Plant
633 Cell 6, 751-759.

634 Fonseca S, Chini A, Hamberg M, Adie B, Porzel A, Kramell R, Miersch O,
635 Wasternack C, Solano R. 2009. (+)-7-iso-Jasmonoyl-L-isoleucine is the
636 endogenous bioactive jasmonate. Nature Chemical Biology 5.

637 Froehlich JE, Itoh A, Howe GA. 2001. Tomato allene oxide synthase and fatty
638 acid hydroperoxide lyase, two cytochrome P450s involved in oxylipin
639 metabolism, are targeted to different membranes of chloroplast envelope. Plant
640 Physiology 125, 306-317.

641 Gilbert NC, Niebuhr M, Tsuruta H, Bordelon T, Ridderbusch O, Dassey A,
642 Brash AR, Bartlett SG, Newcomer ME. 2008. A covalent linker allows for
643 membrane targeting of an oxylipin biosynthetic complex. Biochemistry 47,
644 10665-10676.

645 Griffiths G. 2015. Biosynthesis and analysis of plant oxylipins. Free Radical
646 Research 49, 565-582.

647 Hoffmann M, Hentrich M, Pollmann S. 2011. Auxin-oxylipin crosstalk:
648 relationship of antagonists. Journal of Integrative Plant Biology 53, 429-445.

649 Hofmann E, Pollmann S. 2008. Molecular mechanism of enzymatic allene oxide
650 cyclization in plants. Plant Physiology and Biochemistry 46, 302-308.

651 Hofmann E, Zerbe P, Schaller F. 2006. The crystal structure of *Arabidopsis*
652 *thaliana* allene oxide cyclase: insights into the oxylipin cyclization reaction.
653 Plant Cell 18, 3201-3217.

654 Jackson DT, Froehlich JE, Keegstra K. 1998. The hydrophilic domain of Tic110,
655 an inner envelope membrane component of the chloroplastic protein
656 translocation apparatus, faces the stromal compartment. Journal of Biological
657 Chemistry 273, 16583-16588.

658 Joyard J, Ferro M, Masselon C, Seigneurin-Berny D, Salvi D, Garin J, Rolland
659 N. 2010. Chloroplast proteomics highlights the subcellular compartmentation of
660 lipid metabolism. Progress in Lipid Research 49, 128-158.

661 Kessler F, Blobel G. 1996. Interaction of the protein import and folding
662 machineries of the chloroplast. Proceedings of the National Academy of
663 Sciences of the United States of America 93, 7684-7689.

664 Laemmli UK. 1970. Cleavage of structural proteins during the assembly of the
665 head of bacteriophage T4. Nature 227, 680-685.

666 Laudert D, Pfannschmidt U, Lottspeich F, Holländer-Czytko H, Weiler EW.
667 1996. Cloning, molecular and functional characterization of *Arabidopsis thaliana*
668 allene oxide synthase (CYP 74), the first enzyme of the octadecanoid pathway
669 to jasmonates. Plant Molecular Biology 31, 323-335.

670 Lee DS, Nioche P, Hamberg M, Raman CS. 2008. Structural insights into the
671 evolutionary paths of oxylipin biosynthetic enzymes. Nature 455, 363-368.

672 Li HM, Moore T, Keegstra K. 1991. Targeting of proteins to the outer envelope
673 membrane uses a different pathway than transport into chloroplasts. The Plant
674 Cell 3, 709-717.

675 Li L, Chang Z, Pan Z, Fu ZQ, Wang X. 2008. Modes of heme binding and
676 substrate access for cytochrome P450 CYP74A revealed by crystal structures
677 of allene oxide synthase. Proceedings of the National Academy of Sciences of
678 the United States of America 105, 13883-13888.

679 Ma Y, Kouranov A, LaSala SE, Schnell DJ. 1996. Two components of the
680 chloroplast protein import apparatus, IAP86 and IAP75, interact with the transit
681 sequence during the recognition and translocation of precursor proteins at the
682 outer envelope. Journal of Cell Biology 134, 315-327.

683 Mwenda CM, Matsuki A, Nishimura K, Koeduka T, Matsui K. 2015. Spatial
684 expression of the Arabidopsis hydroperoxide lyase gene is controlled differently
685 from that of the allene oxide synthase gene, J Plant Interactions 10(1), 1-10,
686 Nilsson AK, Fahlberg P, Johansson ON, Hamberg M, Andersson MX,
687 Ellerström M. 2016. The activity of HYDROPEROXIDE LYASE 1 regulates
688 accumulation of galactolipids containing 12-oxo-phytodienoic acid in
689 Arabidopsis. Journal of Experimental Botany 67, 5133-5144.

690 Oldham ML, Brash AR, Newcomer ME. 2005a. Insights from the X-ray crystal
691 structure of coral 8R-lipoxygenase: calcium activation via a C2-like domain and
692 a structural basis of product chirality. Journal of Biological Chemistry 280,
693 39545-39552.

694 Oldham ML, Brash AR, Newcomer ME. 2005b. The structure of coral allene
695 oxide synthase reveals a catalase adapted for metabolism of a fatty acid
696 hydroperoxide. Proceedings of the National Academy of Sciences of the United
697 States of America 102, 297-302.

698 Otto M, Naumann C, Brandt W, Wasternack C, Hause B. 2016. Activity
699 Regulation by Heteromerization of Arabidopsis Allene Oxide Cyclase Family
700 Members. Plants 5.

701 Palatnik JF, Allen E, Wu X, Schommer C, Schwab R, Carrington JC, Weigel D.
702 2003. Control of leaf morphogenesis by microRNAs. Nature 425, 257-263.

703 Park JH, Halitschke R, Kim HB, Baldwin IT, Feldmann KA, Feyereisen R. 2002.
704 A knock-out mutation in allene oxide synthase results in male sterility and
705 defective wound signal transduction in *Arabidopsis* due to a block in jasmonic
706 acid biosynthesis. The Plant Journal 31, 1-12.

707 Reinbothe C, Springer A, Samol I, Reinbothe S. 2009. Plant oxylipins: role of
708 jasmonic acid during programmed cell death, defence and leaf senescence.
709 The FEBS Journal 276, 4666-4681.

710 Reinbothe S, Reinbothe C, Heintzen C, Seidenbecher C, Parthier B. 1993a. A
711 methyl jasmonate-induced shift in the length of the 5' untranslated region
712 impairs translation of the plastid rbcL transcript in barley. The EMBO Journal
713 12, 1505-1512.

714 Reinbothe S, Reinbothe C, Parthier B. 1993b. Methyl jasmonate-regulated
715 translation of nuclear-encoded chloroplast proteins in barley (Hordeum vulgare
716 L. cv. salome). Journal of Biological Chemistry 268, 10606-10611.

717 Rizo J, Südhof TC. 1998. C2-domains, structure and function of a universal
718 Ca2+-binding domain. Journal of Biological Chemistry 273, 15879-15882.

719 Rustgi S, Pollmann S, Buhr F, Springer A, Reinbothe C, von Wettstein D,
720 Reinbothe S. 2014. JIP60-mediated, jasmonate- and senescence-induced
721 molecular switch in translation toward stress and defense protein synthesis.
722 Proceedings of the National Academy of Sciences 111, 14181-14186.

723 Schaller A, Stintzi A. 2009. Enzymes in jasmonate biosynthesis - structure,
724 function, regulation. Phytochemistry 70, 1532-1538.

725 Schaller F, Zerbe P, Reinbothe S, Reinbothe C, Hofmann E, Pollmann S. 2008.
726 The allene oxide cyclase family of Arabidopsis thaliana: localization and
727 cyclization. FEBS Journal 275, 2428-2441.

728 Schnell DJ, Kessler F, Blobel G. 1994. Isolation of components of the
729 chloroplast protein import machinery. Science 266, 1007-1012.

730 Schommer C, Palatnik JF, Aggarwal P, Chetelat A, Cubas P, Farmer EE, Nath
731 U, Weigel D. 2008. Control of jasmonate biosynthesis and senescence by
732 miR319 targets. PLoS Biology 6, e230.

733 Schweizer F, Fernandez-Calvo P, Zander M, Diez-Diaz M, Fonseca S, Glauser
734 G, Lewsey MG, Ecker JR, Solano R, Reymond P. 2013. Arabidopsis basic
735 helix-loop-helix transcription factors MYC2, MYC3, and MYC4 regulate
736 glucosinolate biosynthesis, insect performance, and feeding behavior. Plant
737 Cell 25, 3117-3132.

738 Seltmann MA, Stingl NE, Lautenschlaeger JK, Krischke M, Mueller MJ, Berger
739 S. 2010. Differential impact of lipoxygenase 2 and jasmonates on natural and
740 stress-induced senescence in Arabidopsis. Plant Physiology 152, 1940-1950.

741 Skrzypczak-Jankun E, Amzel LM, Kroa BA, Funk MO, Jr. 1997. Structure of
742 soybean lipoxygenase L3 and a comparison with its L1 isoenzyme. Proteins 29,
743 15-31.

744 Song WC, Brash AR. 1991. Investigation of the allene oxide pathway in the
745 coral *Plexaura homomalla*: formation of novel ketols and isomers of

746 prostaglandin A2 from 15-hydroxyeicosatetraenoic acid. Archives of
747 Biochemistry and Biophysics 290, 427-435.

748 Spivey HO, Ovádi J. 1999. Substrate Channeling. Methods 19, 306-321.

749 Springer A, Kang C, Rustgi S, von Wettstein D, Reinbothe C, Pollmann S, Rein-
750 bothe S. 2016. Programmed chloroplast destruction during leaf senescence in-
751 volves 13-lipoxygenase (13-LOX). Proc Natl Acad Sci USA 113(12):3383-3388.
752 Staswick PE, Su W, Howell SH. 1992. Methyl jasmonate inhibition of root
753 growth and induction of a leaf protein are decreased in an *Arabidopsis thaliana*
754 mutant. Proceedings of the National Academy of Sciences of the United States
755 of America 89, 6837-6840.

756 Stenzel I, Otto M, Delker C, Kirmse N, Schmidt D, Miersch O, Hause B,
757 Wasternack C. 2012. ALLENE OXIDE CYCLASE (AOC) gene family members
758 of Arabidopsis thaliana: tissue- and organ-specific promoter activities and in
759 vivo heteromerization. Journal of Experimental Botany 63, 6125-6138.

760 Thines B, Katsir L, Melotto M, Niu Y, Mandaokar A, Liu G, Nomura K, He SY,
761 Howe GA, Browse J. 2007. JAZ repressor proteins are targets of the $SCF^{COI1}$
762 complex during jasmonate signalling. Nature 448, 661-665.

763 Tijet N, Brash AR. 2002. Allene oxide synthases and allene oxides.
764 Prostaglandins Other Lipid Mediat 68-69, 423-431.

765 Towbin H, Staehelin T, Gordon J. 1979. Electrophoretic transfer of proteins from
766 polyacrylamide gels to nitrocellulose sheets: procedure and some applications.
767 Proceedings of the National Academy of Sciences of the United States of
768 America 76, 4350-4354.

769 von Malek B, van der Graaff E, Schneitz K, Keller B. 2002. The Arabidopsis
770 male-sterile mutant *dde2-2* is defective in the *ALLENE OXIDE SYNTHASE*
771 gene encoding one of the key enzymes of the jasmonic acid biosynthesis
772 pathway. Planta 216, 187-192.

773 Walter M, Chaban C, Schütze K, Batistic O, Weckermann K, Näke C, Blazevic
774 D, Grefen C, Schumacher K, Oecking C, Harter K, Kudla J. 2004. Visualization
775 of protein interactions in living plant cells using bimolecular fluorescence
776 complementation. The Plant Journal 40, 428-438.

777 Wasternack C, Hause B. 2013. Jasmonates: biosynthesis, perception, signal
778 transduction and action in plant stress response, growth and development. An
779 update to the 2007 review in Annals of Botany. Annals of Botany 111, 1021-
780 1058.

781 Wu J, Baldwin IT. 2010. New insights into plant responses to the attack from
782 insect herbivores. Annual Review of Genetics 44, 1-24.

783 Xie DX, Feys BF, James S, Nieto-Rostro M, Turner JG. 1998. COI1: an
784 Arabidopsis gene required for jasmonate-regulated defense and fertility.
785 Science 280, 1091-1094.

786 Yan J, Zhang C, Gu M, Bai Z, Zhang W, Qi T, Cheng Z, Peng W, Luo H, Nan F,
787 Wang Z, Xie D. 2009. The *Arabidopsis* CORONATINE INSENSITIVE1 protein is
788 a jasmonate receptor. The Plant Cell 21, 2220-2236.

789 Yan Y, Borrego E, Kolomiets MV. 2013. Jasmonate Biosynthesis, Perception
790 and Function in Plant Development and Stress Responses. In: Baez RV, ed.
791 *Lipid Metabolism*. Rijeka: InTech, Ch. 16.

792 Youn B, Sellhorn GE, Mirchel RJ, Gaffney BJ, Grimes HD, Kang C. 2006.
793 Crystal structures of vegetative soybean lipoxygenase VLX-B and VLX-D, and
794 comparisons with seed isoforms LOX-1 and LOX-3. Proteins: Structure,
795 Function, and Bioinformatics 65, 1008-1020.

796 Zerbe P, Weiler EW, Schaller F. 2007. Preparative enzymatic solid phase
797 synthesis of cis(+)-12-oxo-phytodienoic acid - physical interaction of AOS and
798 AOC is not necessary. Phytochemistry 68, 229-236.

799

800

## FIGURE LEGENDS

**Figure 1.** The Vick and Zimmerman pathway leading to JA and the concurrent AOS and HPL reactions. Pathway intermediates are abbreviated as follows: 13-HPOT, (9*Z*11*E*15*Z*13*S*)-13-hydroperoxy-9,11,15-octadecatrienoic acid; EOT, 12,13(*S*)-epoxy-9(*Z*),11,15(*Z*)-octadecatrienoic acid; OPDA, *cis*-(+)-12-oxophytodienoic acid; ODA, 12-oxo-*cis*-9-dodecenoic acid. The enzymes are indicated as follows: LOX, 13-lipoxygenase; AOS, allene oxide synthase; AOC, allene oxide cyclase; HPL, hydroperoxy lyase. Note that EOT is short-lived and spontaneously disintegrates into volatile α-ketols and γ-ketols as well as racemic OPDA.

**Figure 2.** *In vitro*-import and differential membrane binding of AOS and HPL in chloroplasts. **(A)** Levels of $^{35}$S-Met-labelled ($^{35}$S)- AOS (a) and $^{35}$S-HPL (b) before and after import into isolated *Arabidopsis* chloroplasts. Thl, thermolysin; TP, translation product. Positions of precursor protein (pAOS and pHPL) and mature protein (AOS, HPL) are indicated. **(B)** Detection by SDS-PAGE and autoradiography of $^{35}$S-AOS (a) and $^{35}$S-HPL (b) in trypsin (Try)-treated (+Try) and untreated (-Try) mixed outer and inner plastid envelopes (ME), inner plastid envelope (IM), outer plastid envelope (OM), thylakoids (Th) and stroma (St). CP defines the chloroplast reference fraction prior to import and protease treatment. The Western blot in panel c shows the levels of TIC110 and TOC75 in non-trypsin-treated chloroplasts (CP) versus trypsin (Try)-treated chloroplasts containing imported $^{35}$S-AOS/HPL and respective subfractions. **(C)** Western blot analysis of TOC75, the translocon at the inner chloroplast envelope membrane protein TIC55, the chlorophyll a/b binding protein LHCII (CAB) and the small subunit of ribulose-1,5-bisphosphate carboxylase/oxygenase (SSU) in the indicated fractions of non-trypsin-treated chloroplasts. Abbreviations are as in B. **(D)** Membrane binding of imported $^{35}$S-AOS (a) and $^{35}$S-HPL (b), as assessed by their extractability by 1 M NaCl and 0.1 M $Na_2CO_3$, pH 11. Both pellet (P) and supernatant (S) fractions, respectively, obtained after sedimentation of the membranes, were tested by SDS-PAGE and autoradiography for the two labeled proteins.

834 **Figure 3.** Detection of AOS complexes *in vitro* and *in planta*. **(A)** Gel filtration
835 elution profile of AOS-Flag in protein extracts of transgenic plants expressing
836 Flag-tagged AOS (solid line) and in isolated chloroplasts after *in vitro*-import of
837 AOS-$(His)_6$ (broken line). Positions of size marker proteins are indicated (squares
838 and dotted line). **(B)** as A, but showing a Western blot analysis of AOS-Flag. $M_r$
839 defines radioactive molecular mass standards. **(C)** SDS-PAGE pattern of plastid
840 envelope proteins co-purifying with AOS-$(His)_6$ (lane 1) and HPL-$(His)_6$ (lane 2).
841 The indicated bands were identified by protein sequencing.
842
843 **Figure 4.** Genetic dissection of LOX2-AOS-AOC2 complex formation. **(A)** Time
844 course of AOS, LOX2 and AOC2 accumulation in wild-type (WT) and *TCP4*
845 plants expressing a mi319-resistant version of TCP4 during development (in
846 weeks [w]). **(B)** as A, but depicting accumulation of AOS, LOX2 and AOC in
847 plants of *jaw*-D, *aoc2*, wild-type (WT), *lox2*, *aos* and *TCP4* backgrounds. **(C)** as
848 A, but showing accumulation of AOS, LOX2 and AOC in plastid envelopes of 4
849 weeks-old *jaw*-D, *coi1*, *jar1* and wild-type (WT) plants after treatment with
850 45 µM MeJA for 24 h. Western blots were simultaneously probed with antisera
851 against LOX2, AOS and AOC2 and developed with either horseradish peroxi-
852 dase-alkaline phosphatase-based (A and B) or enhanced chemiluminescence-
853 based (C) detection systems.
854
855 **Figure 5.** Channeling of jasmonate precursors in the LOX2-AOS-AOC2 plastid
856 envelope complex. **(A)** Label-transfer crosslinking by $^{125}$I-APDP–LOX2, $^{125}$I-
857 APDP–AOS and $^{125}$I-APDP–AOC2 of proteins in mixed outer and inner enve-
858 lopes of *Arabidopsis* chloroplasts. **(B)** Time course of *cis*-(+)-12-OPDA for-
859 mation from α-LeA (filled circles) and 13-HPOT (filled triangles) by the isolated
860 envelope complex containing LOX2, AOS and AOC2. For comparison, *cis*-(+)-
861 12-OPDA formation from α-LeA was tested in the presence of vernolic acid
862 (VA)(open circles). **(C)** Rate of *cis*-(+)-12-OPDA formation determined after
863 10 min incubations for α-LeA (lanes a and e) and 13-HPOT (lanes c and g) by
864 virtue of the LOX2-AOS-AOC2 envelope complex (lanes a-d), as compared to
865 free enzymes released from the membrane complex by treatment with 3% SDS
866 and dialyzed before analysis (lanes e-h, respectively). Respective controls show

867 incubations performed with vernolic acid (VA)(lanes b, d and f and h, respec-
868 tively). Error bars refer to three independent experiments.
869
870 **Figure 6.** Genetic dissection of AOS-LOX2-AOX2 interactions in the split-ubiq-
871 uitin system. Experiments were performed employing fusions to the C- (Cub)
872 and N-terminal (NubG) halves of ubiquitin. Alg5-NubI, the fusion of the unre-
873 lated ER membrane protein Alg5 to NubI, was used as positive control. Nega-
874 tive controls were fusions of Alg5 to Cub or NubG (Alg5-Cub and Alg5-NubG).
875 Qualitative estimation of interactions was deduced from the growth behavior of
876 co-transformed yeast cells on solidified selection medium, while for quantitative
877 assays the ß-galactosidase activity of cells grown in liquid culture was analyzed.
878
879 **Figure 7.** Structural model of the LOX2-AOS-$(AOC2)_3$ interaction in the chloro-
880 plast inner envelope. Trans-membrane domain was shown in orange. Active
881 site residues are shown by shears, and interacting residues by line. Active site
882 predictions for LOX2 are based on Youn et al. (2006), for AOS2 on Lee et al.
883 (2008) and for AOC2 on Hofmann et al. (2006) and trans-membrane domain
884 predications are based on TMpred for LOX2 and $(AOC2)_3$.
885

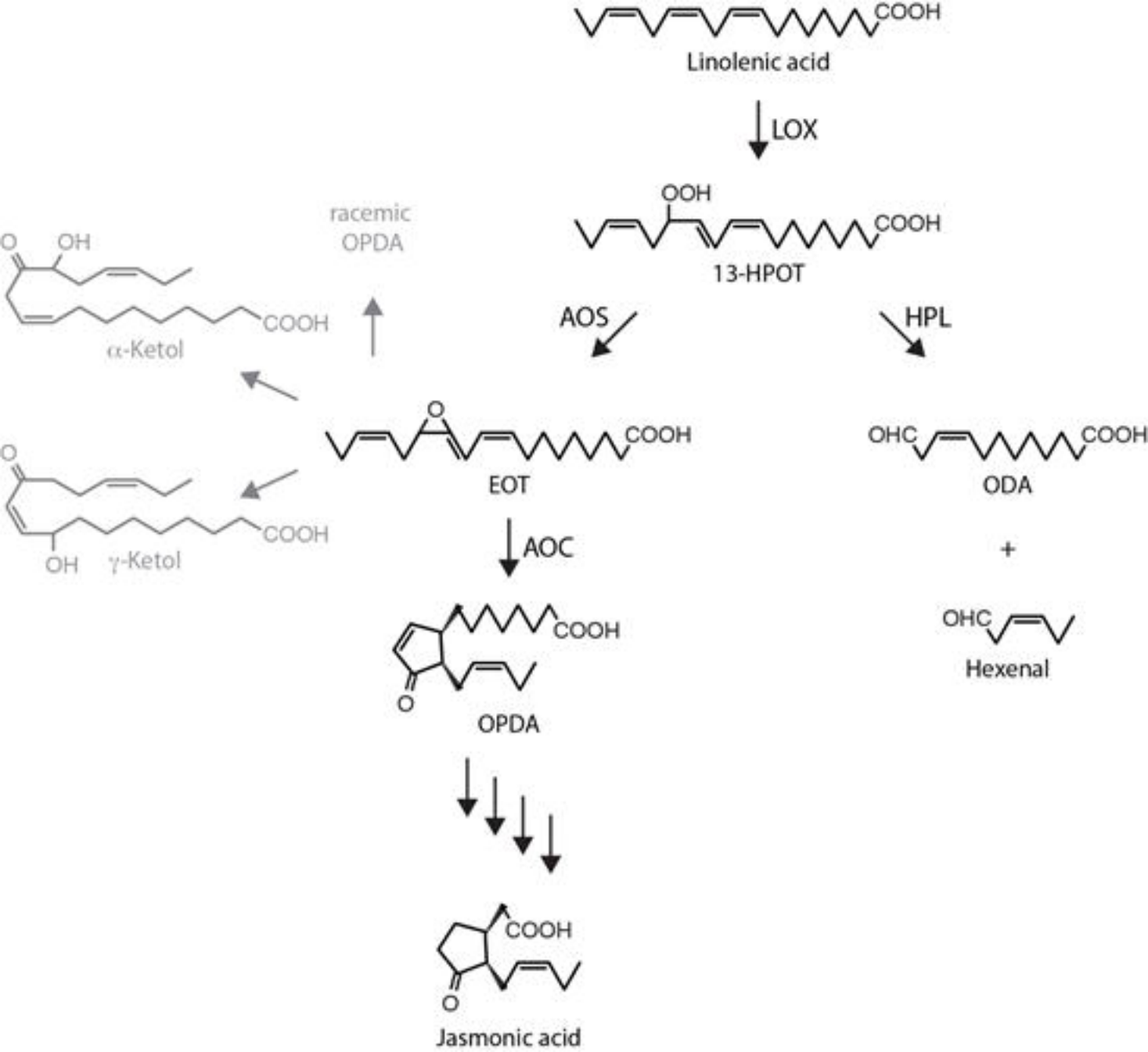
COOH
Linolenic acid
LOX
OOH
COOH
13-HPOT
AOS
HPL
racemic
OPDA
O
OH
COOH
α-Ketol
O
COOH
EOT
OHC
COOH
ODA
+
O
COOH
OH
γ-Ketol
AOC
COOH
O
OPDA
OHC
Hexenal
COOH
O
Jasmonic acid

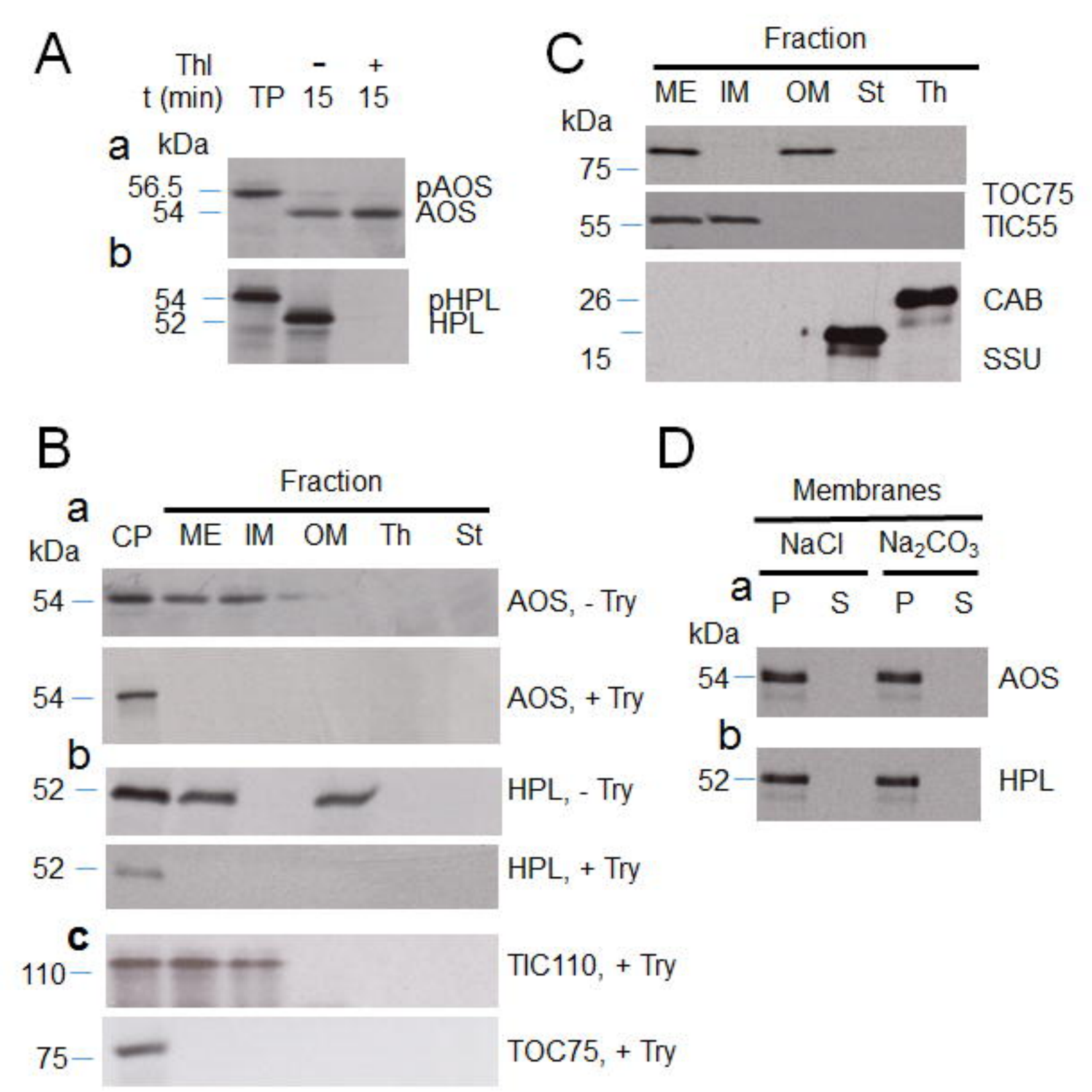
A
Thl
t (min)
TP
-
15
+
15
a
kDa
56.5
54
pAOS
AOS
b
54
52
pHPL
HPL
C
Fraction
ME
IM
OM
St
Th
kDa
75
55
26
15
TOC75
TIC55
CAB
SSU
B
Fraction
a
CP
ME
IM
OM
Th
St
kDa
54
AOS, - Try
54
AOS, + Try
b
52
HPL, - Try
52
HPL, + Try
c
110
TIC110, + Try
75
TOC75, + Try
D
Membranes
NaCl
Na2CO3
a
P
S
P
S
kDa
54
AOS
b
52
HPL

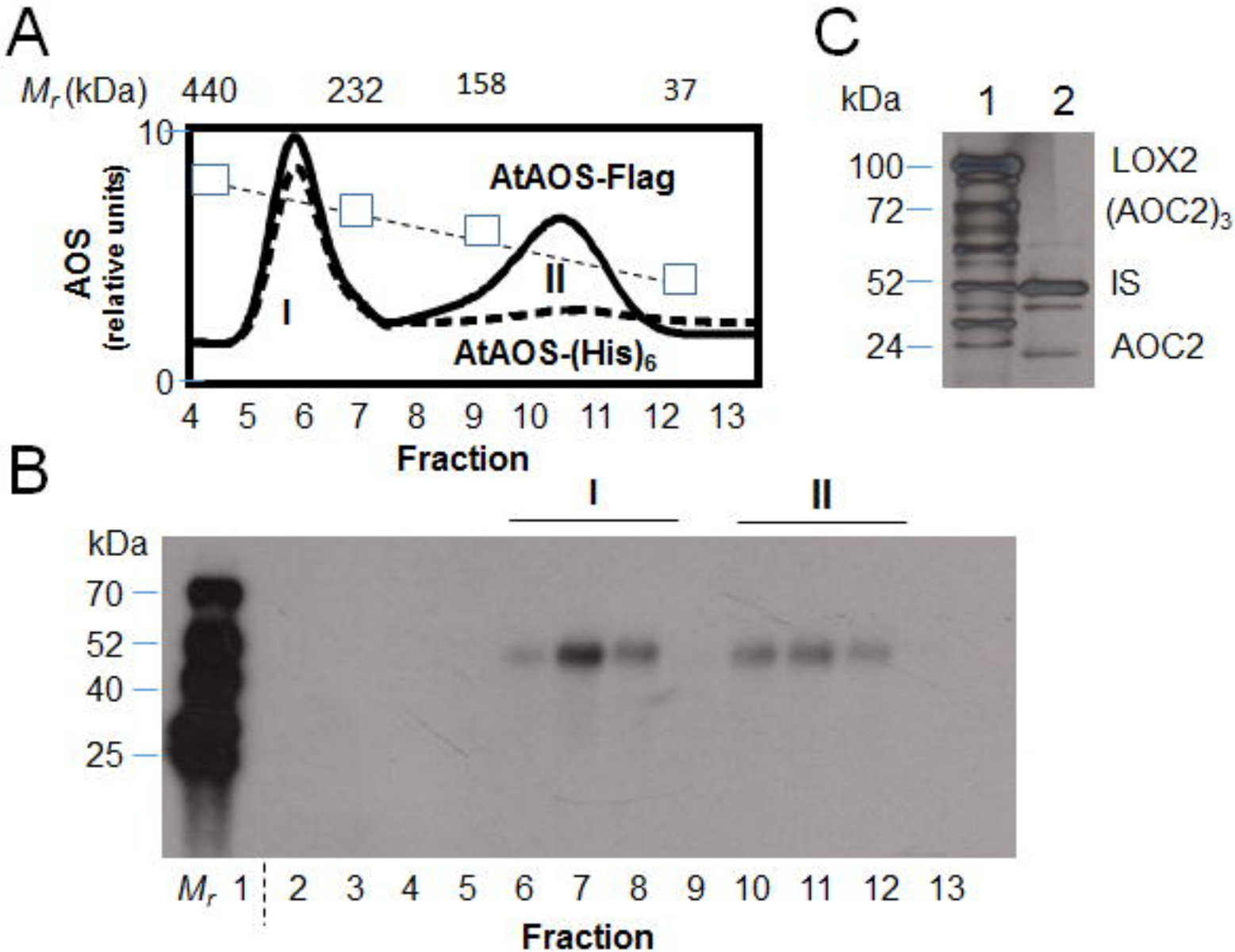
A
$M_r$ (kDa)
440
232
158
37
10
0
AOS
(relative units)
AtAOS-Flag
AtAOS-(His)6
I
II
4 5 6 7 8 9 10 11 12 13
Fraction
C
kDa
1
2
100
72
52
24
LOX2
(AOC2)3
IS
AOC2
B
I
II
kDa
70
52
40
25
$M_r$ 1 2 3 4 5 6 7 8 9 10 11 12 13
Fraction

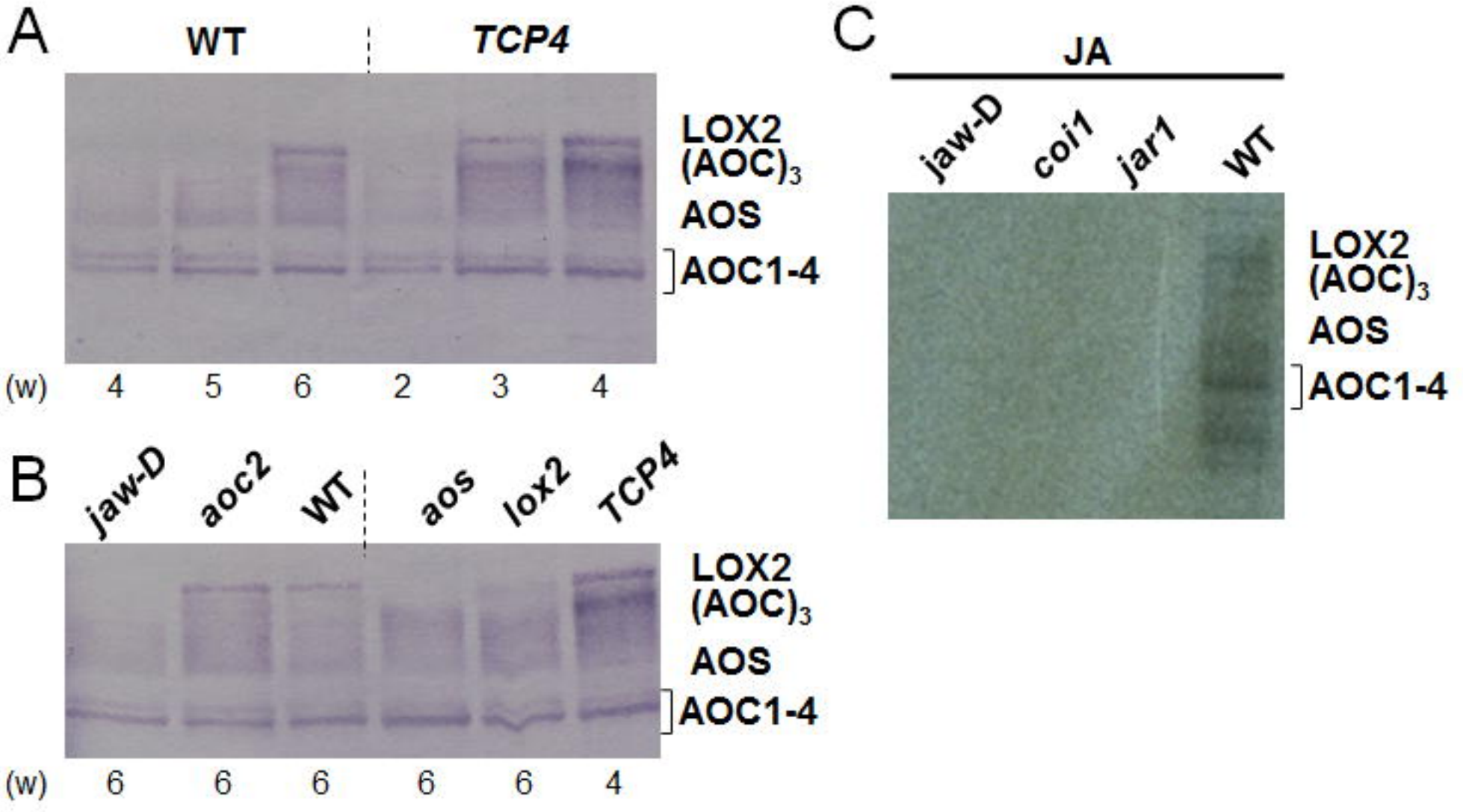
A
WT
TCP4
LOX2
(AOC)3
AOS
AOC1-4
(w)
4
5
6
2
3
4
B
jaw-D
aoc2
WT
aos
lox2
TCP4
LOX2
(AOC)3
AOS
AOC1-4
(w)
6
6
6
6
6
4
C
JA
jaw-D
coi1
jar1
WT
LOX2
(AOC)3
AOS
AOC1-4

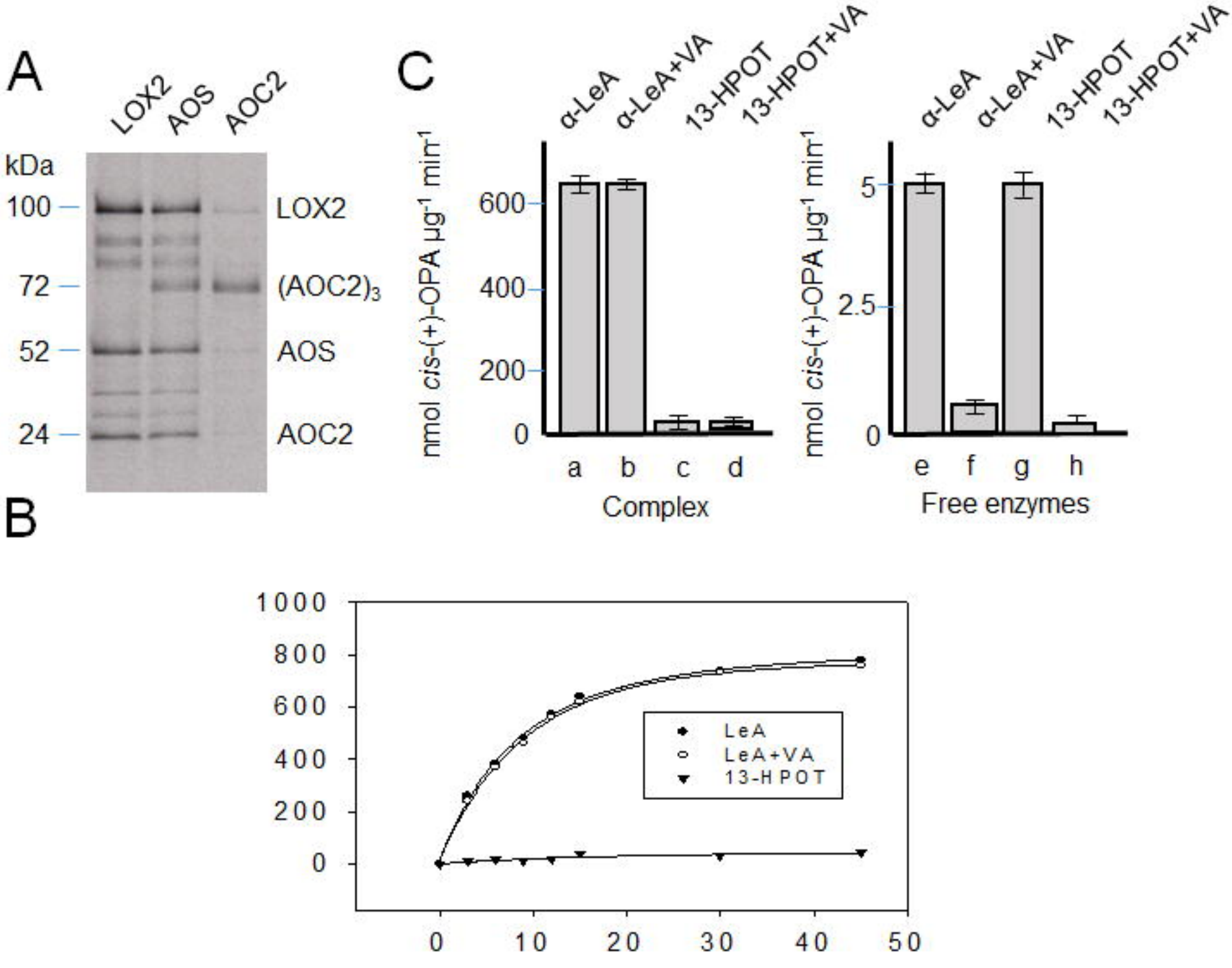
A
LOX2
AOS
AOC2
kDa
100
72
52
24
LOX2
(AOC2)3
AOS
AOC2
C
α-LeA
α-LeA+VA
13-HPOT
13-HPOT+VA
nmol cis-(+)-OPA µg-1 min-1
600
400
200
0
a
b
c
d
Complex
5
2.5
0
e
f
g
h
Free enzymes
B
1000
800
600
400
200
0
0
10
20
30
40
50
LeA
LeA+VA
13-HPOT

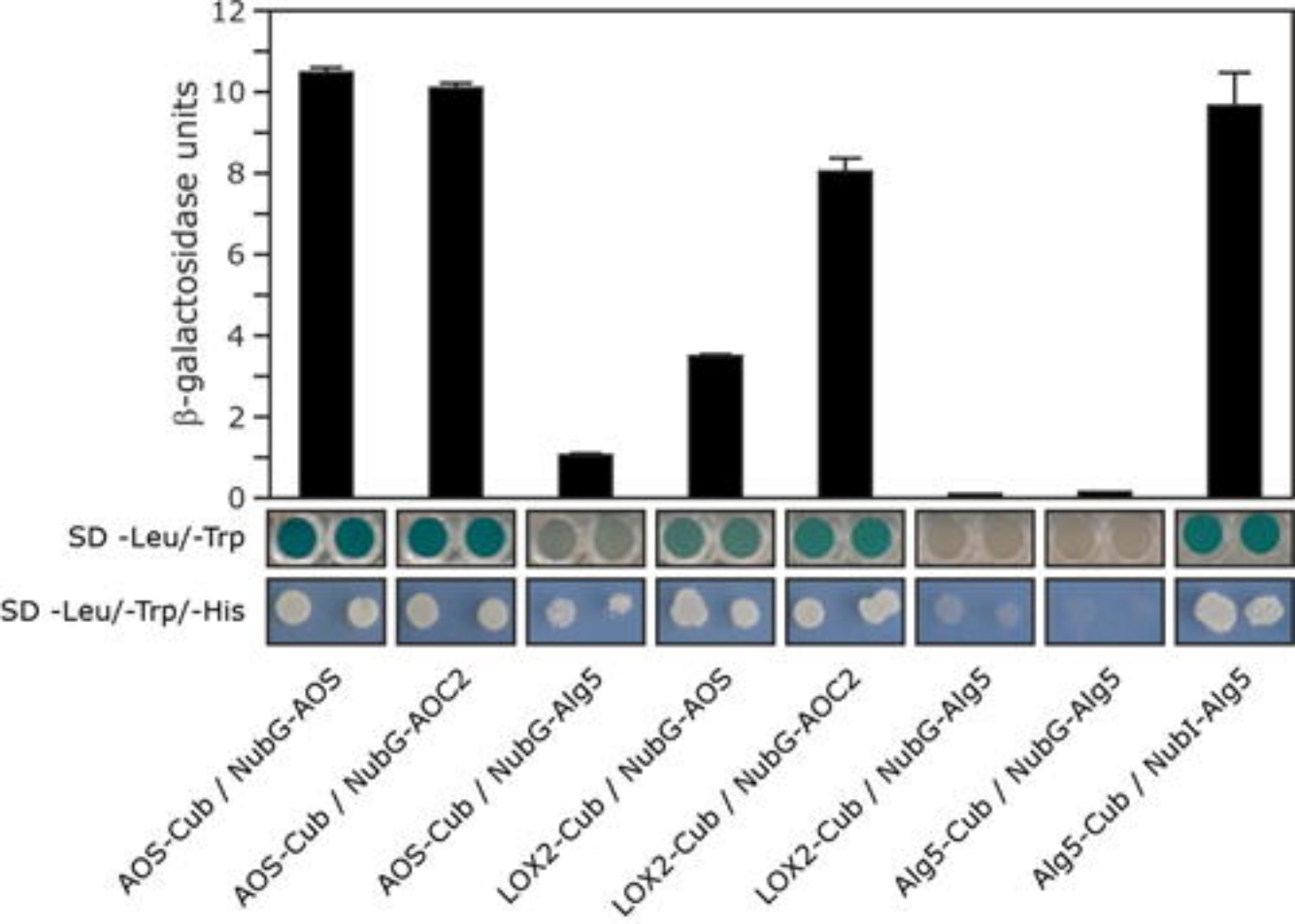
β-galactosidase units
12
10
8
6
4
2
0
SD -Leu/-Trp
SD -Leu/-Trp/-His
AOS-Cub / NubG-AOS
AOS-Cub / NubG-AOC2
AOS-Cub / NubG-Alg5
LOX2-Cub / NubG-AOS
LOX2-Cub / NubG-AOC2
LOX2-Cub / NubG-Alg5
Alg5-Cub / NubG-Alg5
Alg5-Cub / NubI-Alg5

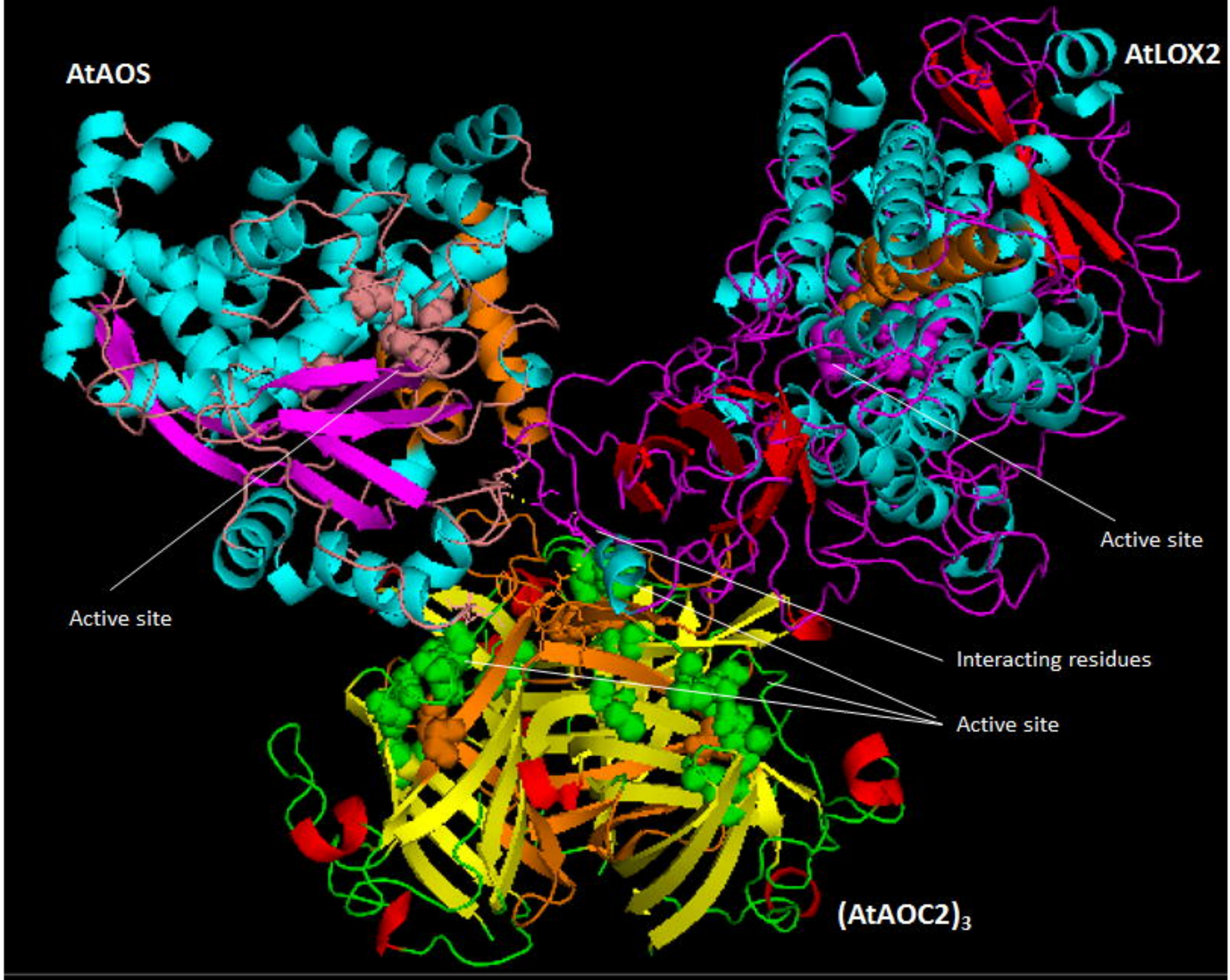
AtAOS
AtLOX2
Active site
Active site
Interacting residues
Active site
$(AtAOC2)_3$